Journal of Ceramic Processing Research. Vol. 14, No. 1, pp. 125~130 (2013)

J O U R N A L O F
Ceramic Processing Research

Influences of two-step calcinations upon the fabrication and morphological control of $Lu_2Ti_2O_7$ powders using oxides as precursors

Bao-rang Li*, Hui Gao, Wei Shang and Zuo-dong Li
School of Energy, Power and Mechanical Engineering, North China Electric Power University, Beijing 102206, P. R. China

Based on observations of the influence of calcination temperature and annealing time on the synthesis of $Lu_2Ti_2O_7$ powders under molten salt conditions, a new route for preparing nano-ceramic powders from oxides, two-step calcinations (TSC), is suggested in this paper. Moreover, the TSC process was investigated in detail using XRD and SEM technologies. Commercial ceramic oxide powders TiO_2 (particle size 20 nm) as well as Lu_2O_3 (particle size 3-4 um) were used as the raw materials and further calcinated with different heating schedules. The results showed that TSC could retard the grain growth and accelerate the phase transformation of $Lu_2Ti_2O_7$ more effectively in comparison with single-step calcination (SSC). By controlling the calcination temperature and time, spherical $Lu_2Ti_2O_7$ powders with nano-sized particles were achieved from oxide precursors by TSC.

Key words: A Powders-solid state reaction, A. Grain growth, A Calcination, B. Grain size.

Introduction

Nanostructures have unique properties, such as phase transition temperatures, melting points and solubilities, which depend on their size [1]. Due to these unique features, a number of chemical methods have been used for synthesizing nano-powders, such as co-precipitation, the sol-gel method, hydrothermal synthesis, combustion and micro-wave-assisted synthesis [2-5], etc. Using these methods, homogeneous products can be obtained, but they require additional heat treatment at higher temperatures to obtain well-crystallized products. In addition, most of these methods suffer from complex and time-consuming procedures and possible mismatch in the solution behavior of the constituents. Molten salt synthesis (MSS) is a process that yields a large amount of ceramic in a relatively short period of time. It has been widely used for the preparation of unitary oxides and multi component oxides [6-8], which can give good reaction conditions with a high ion concentration and rapid pervasion. In recent years, this technique has also been used for synthesizing the desirable nano-sized powders [9-14]. However, oxides have seldom found to be used as the starting precursors in these reports. Lutetium titanium oxide ($Lu_2Ti_2O_7$) has a pyrochlore structure and is particularly suitable for application in an optical imaging system due to its high refractive index and high density. To our knowledge, although different synthesis routes have been studied in order to obtain $Lu_2Ti_2O_7$ particles in the sub-micrometre range [15-19], there have been few reports on the preparation of $Lu_2Ti_2O_7$ oxides from molten salts. In our previous study, we reported a new modified method, two-step-calcinations (TSC) assisted molten salt method, by which well-dispersed $Lu_2Ti_2O_7$ nano-powders were directly synthesized from the oxides precursors [20]. So in the present paper, a detailed investigation of TSC is reported.

*Corresponding author:
Tel : +86-010-6177-2355
Fax: +86-010-6177-2383
E-mail: libr@ncepu.edu.cn

Experimental Procedure

In the present study commercial ceramic oxide powders of TiO_2 and Lu_2O_3 were used as the raw materials, which were of AR grade. The TiO_2 powder was spherical and slightly agglomerated with an average particle size of 20 nm. The Lu_2O_3 powders were rectangular and about 3-4 μm in size. A powder mixture of these raw materials according to the stoichiometric ratio of $Lu_2Ti_2O_7$ was prepared for reaction. NaCl was chosen as the solvent. The prepared reactant and the solvent with a mole ratio of 5:1 were mixed and ball-milled in an ethanol medium. After ball milling, the slurry obtained was dried at 80 °C to remove the ethanol. For TSC, samples were heated in a muffle furnace with a heating rate of 10 $Kminute^{-1}$ to the desired temperature T1, and then rapidly cooled down to T2 with a cooling rate of 30 $Kminutes^{-1}$. The detailed heating procedures of the samples are presented in Fig. 1. After the heat treatment, the products were washed using hot deionized water to remove the residual salt. The products were then dried and characterized using an X-ray diffractometer (XRD, D/max-RB, Japan) for the phase composition and a scanning electron microscope (SEM, Model JSM-6700, JEOL, Japan) for the particle morphology. To quantify the fraction of the $Lu_2Ti_2O_7$ phase, the following equation was used:

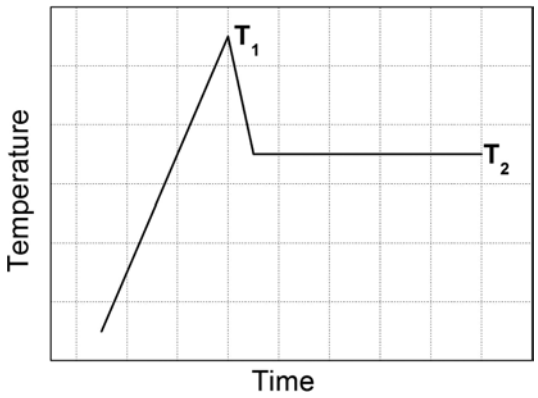

Fig. 1. Sintering schedules for calcination of the samples.

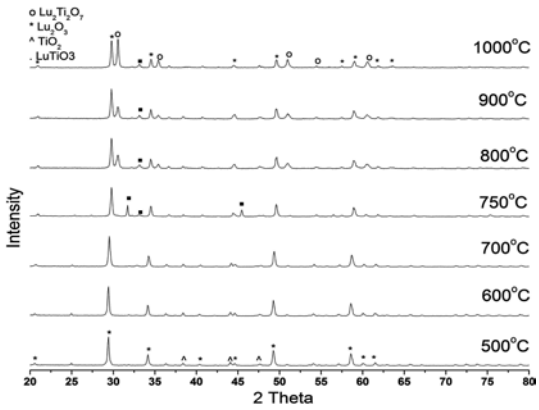

Fig. 2. XRD patterns of the synthesized powder in a NaCl flux calcined at different temperatures.

$$fraction(\%) = \frac{\sum I_{LTO(hkl)}}{\sum I_{(hkl)}} \quad (1)$$

where $I_{LTO(hkl)}$ are the intensities of the diffraction peaks of $Lu_2Ti_2O_7$.

Results and Discussions

Single-step calcinations (SSC)

The XRD patterns of the samples synthesized at temperatures ranging from 500 to 1100 °C are shown in Fig. 2. The holding time was 4h. It is clear that at temperatures lower than 750 °C only TiO_2 and Lu_2O_3 can be found. The intermediate phase such as $LuTiO_3$ besides the TiO_2 phase and traces of Lu_2O_3 is present in the sample synthesized at 750 °C. Although pure $Lu_2Ti_2O_3$ phase is not formed at this temperature, formation of the intermediate phase indicates that the synthesis reactions among the starting materials have been triggered. After heat treatment at 800 °C, the $Lu_2Ti_2O_7$ phase, in addition to TiO_2 and Lu_2O_3, starts to form in the sample. When the temperature is increased to 900 °C, the amount of the $Lu_2Ti_2O_7$ phase is gradually increased. The intensities of the diffraction peaks corresponding to $Lu_2Ti_2O_7$ strengthen with increasing temperature, especially for the diffraction peak (222) occurring near $2\theta = 30.75$ °, which indicates that a better crystallization can be obtained at a higher temperature. By increasing the temperature to 1000 °C, the peak intensities of $Lu_2Ti_2O_7$ are obviously more than of the other phases while at the same time only smaller amounts of the TiO_2 and Lu_2O_3 phases are left with $Lu_2Ti_2O_7$ as the main phase. It has been reported that the conventional solid-state synthesis of the pure $Lu_2Ti_2O_7$ phase was virtually impossible at a temperature lower than 1100 °C. Moreover, TiO_2 and Lu_2O_3 phases were reported to be present with the formation of $Lu_2Ti_2O_7$ [18, 19]. The pure $Lu_2Ti_2O_7$ phase can only be obtained at temperatures higher than 1100 °C. This is very similar to our studies.

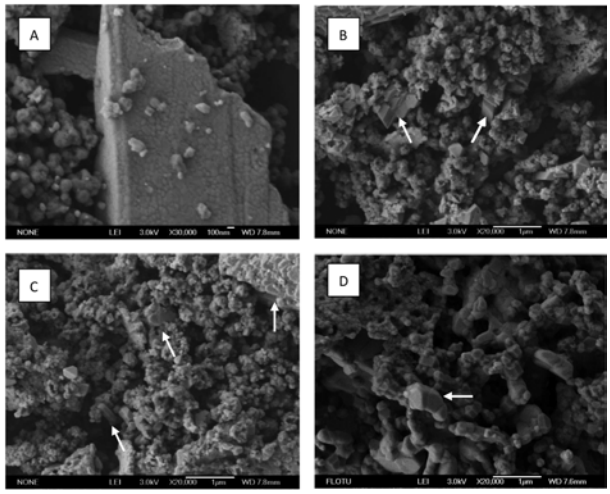

Fig. 3. SEM micrographs of $Lu_2Ti_2O_7$ powders synthesized at different temperatures (A) 750 °C; (B) 800 °C; (C) 1000 °C; (D) 1100 °C.

Fig. 3 shows SEM micrographs of $Lu_2Ti_2O_7$ powders synthesized at different temperatures. It is observed that both the grain size and crystal morphologies of powders changes greatly with an increment of temperature to 1100 °C. As can be seen in Fig. 3 (A), the powders synthesized at 750 °C are mainly composed of spherical particles with an average grain size less than 100 nm. Obvious agglomeration in large blocks shown in Fig. 3 (A), can be observed. No pure $Lu_2Ti_2O_7$ phase is synthesized at this temperature. This observation is consistent with XRD results shown in Fig. 2. The melting point of NaCl is approached at 800 °C. So the starting materials should still be in a simple mixed state at 750 °C. The triggered synthesis reaction is similar to that in the solid phase reaction from the mixture of oxides. At this stage the product morphology is similar to that of TiO_2 in the reactants which acts as a template in the further synthesis process [9]. As the temperature is increased to 800 °C-1000 °C, abnormal grain growth can be observed (as shown by arrows). The large sized grain with perfect crystal faces are about 200-400 nm while the small particles are still spherical in shape, which is similar to that of Fig. 3 (A). With a further increase of temperature up to 1100 °C, the crystal edges of the large particles become round and the shape of the particles is irregular, which indicates the beginning

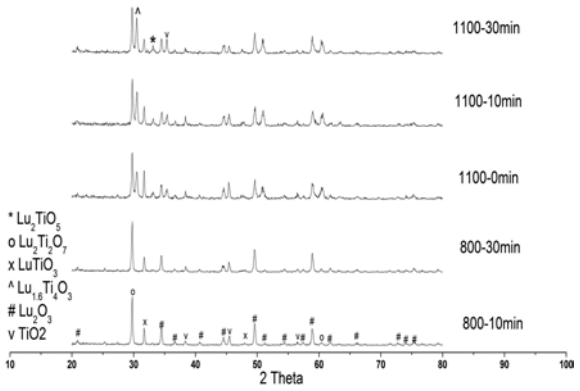

Fig. 4. XRD patterns of the powders calcinated at different temperatures with different times.

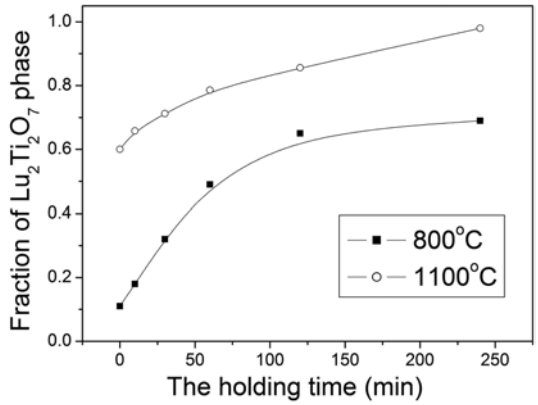

Fig. 5. Dependence of the phase transformation ratio on the calcination time.

of a decrease in crystalline perfection. Moreover, a duplex microstructure with small agglomerated grains of less than 100 nm and abnormally large grains in the range of 500 nm becomes clear. Another phenomenon found in Fig. 3 is that the smaller particle sizes seem to decrease with the increased temperature although no obvious changes are found in the shape of the smaller particles. This suggests the amount of small particles might have a close relation to the annealing temperature.

Effects of the holding time

In order to find the influence of the holding time on the phase transformation and particle morphology, the precursors are calcined at different temperatures with holding times ranging from 0 minute to 4 h. XRD patterns of the powders obtained are shown in Fig. 4. After annealing for 30 minutes at 800 °C, Fig. 4 indicates large amounts of Lu_2O_3 and TiO_2 are still found although the sharp peaks corresponding to $Lu_2Ti_2O_7$ and $LuTiO_3$ are also observed. In comparison with Fig. 2 (800 °C sample), it is easily seen that the intermediate phase formed gradually disappears with a prolonged annealing time indicating that the annealing time is helpful in the phase transformation. This also can be observed more clearly at higher temperature such as 1100 °C. When the annealing time is less than

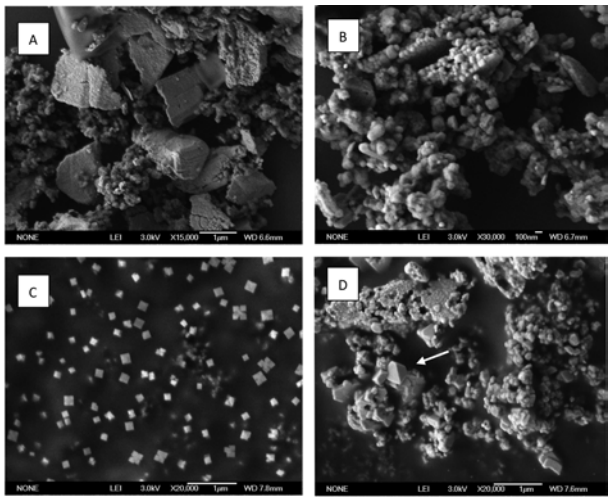

Fig. 6. SEM micrographs of $Lu_2Ti_2O_7$ powders synthesized at different temperatures (A) 800 °C/30 minutes; (B) 800 °C/120 minutes; (C) 1100 °C/10 minutes; (D) 1100 °C/30 minutes.

30 minutes, Fig. 4 shows type of the intermediate phase formed at 1100 °C are more than that obtained at 800 °C. The other intermediate phases such as Lu_2TiO_5, $Lu_{1.6}Ti_4O_3$, etc are also found besides $LuTiO_3$. However, with a further increasing in the holding time, all the intermediate phases disappear gradually.

For clarity, the dependence of the phase transformation ratio on the calcinations time is shown in Fig. 5. It is easily seen from Fig. 5 that the amount of $Lu_2Ti_2O_7$ increases with an increasing in the holding time, especially when the prolonged time is within 2 h. The above results indicate that the holding time is also a crucial factor to facilitate phase transformation besides the temperature. So a prolonged holding time is helpful for the formation of $Lu_2Ti_2O_7$. But at the same time a longer holding time also contributes to particle growth resulting in the formation of abnormally large particles, which can be observed in Fig. 6. Fig. 6 shows the microstructures of samples as a function of temperature and holding time. At a low temperature, no obviously abnormal particle growth is found in the samples. However, Fig. 5 indicates a low temperature also leads to a low fraction of the $Lu_2Ti_2O_7$ phase in samples and the amount of $Lu_2Ti_2O_7$ phase increases with an increase of the calcination temperature. At an elevated temperature with sufficient holding time, almost 100% of the $Lu_2Ti_2O_7$ phase can be obtained, but at the same time abnormal particle growth is also generated. For example a duplex microstructure is formed when the calcination time is above 30 minutes at 1100 °C. Although the large particles can be avoided by shortening the holding time, this is usually achieved in the experiment at the sacrifice of $Lu_2Ti_2O_7$ formation.

Investigations on TSC

In order to have an effective control of the particle morphology and avoid the formation of a duplex microstructure, both an increased temperature and a

Table 1. The selected combinations of T1 and T2 of the samples.

T1 (°C)	T2 (°C)	Sample	Fraction $Lu_2Ti_2O_7$	of Abnormal. phase Growth (%)
1100	900	A1	> 98	Y
	850	A2	> 98	Y
	800	A3	> 98	N
	750	A4	80-90	N
1000	900	A5	> 95	N
	850	A6	> 95	N
	800	A7	> 88	N
	750	A8	< 75	N
950	800	A9	40-50	N
	750	A10	20-30	N

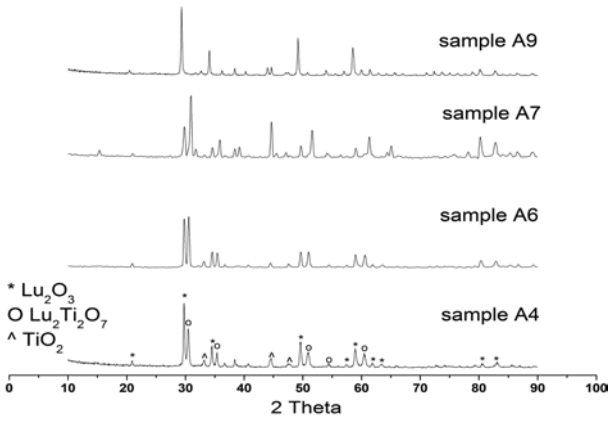

Fig. 7. XRD patterns of the samples under TSC conditions.

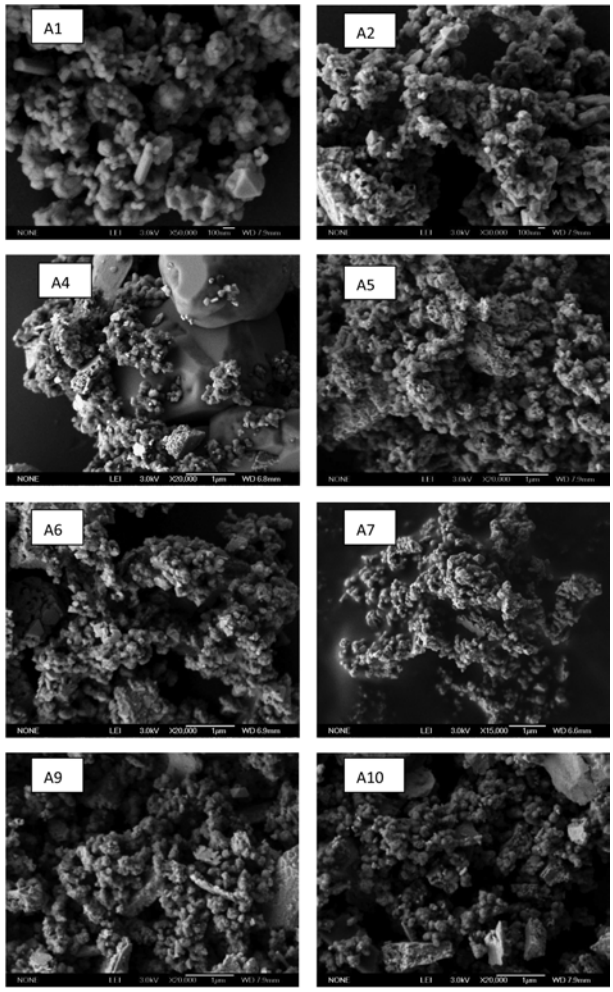

Fig. 8. SEM micrographs of the samples under TSC conditions.

shortened holding time become necessary. To achieve this, the sample is first heated to a higher temperature then cooled down to a lower temperature to suppress particle growth, and held at that temperature until the full phase transition [20].

In order to make detailed investigations of TSC, the temperatures of the first calcination step for $Lu_2Ti_2O_7$ (T1) were chosen as 1100, 1000 and 900 °C. The temperature of the second calcination step (T2) is lower than T1; the decrease from T1 to T2 is tested in the range of 100-350 °C. The selected combinations of T1 and T2 of the samples are given in Table 1. Fig. 7 is the XRD patterns of the samples presented in Table 1. According to equation 1, the calculated fractions of the $Lu_2Ti_2O_7$ phase are also shown in Table 1.

In the single-step sintering runs at the temperature of T1, the maximum fraction of the $Lu_2Ti_2O_7$ phase reaches 10.0-60.1% corresponding to the peak temperature of 800-1100 °C for 0 minute. In the single-step sintering runs at a temperature of T2, the fraction of the $Lu_2Ti_2O_7$ phase varies between 32% and 71.2% when calcined at 800-1100 °C for 30 minutes. So it is impossible to achieve pure $Lu_2Ti_2O_7$ merely by calcining the samples at temperatures below 1100 °C for 30 minutes. However, when an adequate peak temperature of T1 is applied before holding the samples at a temperature of T2, pure $Lu_2Ti_2O_7$ is achieved at the same temperature and with the same holding time of 30 minutes. Just as is shown in table 1, in the TSS process, a high fraction of the $Lu_2Ti_2O_7$ phase is generally achieved in samples A1, A2, A3, A5 and A6 while a relatively low fraction of $Lu_2Ti_2O_7$ phase is found in samples A4, A7, A8, A9 and A10. For example the fractions of the $Lu_2Ti_2O_7$ phase in samples A1, A2, A3, A5 and A6 are higher than 95% while that of sample A8 is less than 75%. These results indicate both an increased T1 and T2 in TSS are effective in promoting a further phase transformation. Fig. 8 shows SEM micrographs of the samples. Fig. 8 suggests a second calcination temperature T2 higher than 850 °C leads to a duplex microstructure when T1 is chosen as 1100 °C. No abnormal particle growth in samples A5, A 6, A9 and A10 is obviously found, which implies both lowered temperatures T1 and T2 are effective to control abnormal particle growth. Based on these observations, it is reasonably concluded that in order to achieve a high fraction of the $Lu_2Ti_2O_7$ phase combined with no abnormal particle growth, both T1 and T2 should be chosen to be as low

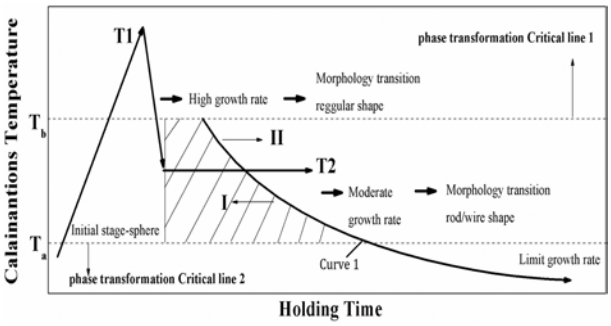

Fig. 9. Influence of temperature and time on the particle morphology evolution.

as possible if no interruption to the phase transition is to be assured and an incomplete phase transformation at T1 due to a lower holding time can be further finished during the subsequent holding process at a temperature of T2.

Based upon the above investigations, a concluded TSC technology is given in Fig. 9 in which two level lines, T_a and T_b, represent the lowest temperature for T1 and T2, respectively when TSC is efficient.

For SSC, at low temperature (for example temperatures lower than T_a in Fig. 9), the corresponding growth rate is limited and the growth rate associated with the facets of the crystal is nearly equal. So, the particle morphology transition cannot be introduced in spite of a longer annealing time, even with the sustained time longer than the curve 1 shown in Fig. 9. At the same time, the phase transformed fraction must be very low, which can be speculated from Fig. 5. However, the increased nucleation and growth rate can lead to an obvious morphological transition if the calcinations temperature is further increased (for example temperatures arranging from Ta to Tb in Fig. 9).

In the process of preparing $Lu_2Ti_2O_7$ powders, molten salt provides an apt solvent environment. In this molten flux, TiO_2 molecules disperse, and then diffuse rapidly throughout the salt in spite of a small solubility while Lu_2O_3 can dissolve effectively in the salt. So the morphology of a $Lu_2Ti_2O_7$ particle is typically spherical in shape, which is similar to that of TiO_2 at the beginning of particle growth upon further heating with the holding time further prolonged at this stage, particles of the $Lu_2Ti_2O_7$ phase tend to change in shape due to the growth process followed. The final shape of $Lu_2Ti_2O_7$ may be determined by various growth rates associated with the facets of the crystal [21]. So, under single step calcinations conditions, one possible case is that the spherical particles formed would change gradually into rod-like particles and in a further step these small rod-like particles would assemble and result in nano-wires with the help of the crystallization habits of the salts under proper conditions in the corresponding temperature range. This is the possible $Lu_2Ti_2O_7$ nano-wire formation mechanism we suggested in our previous studies [22]. From Fig. 9, it is also easily seen that the fast growth and nucleation rate resulting from a high temperature ($> T_b$) usually produces large particles with an irregular shape [23].

For two step calcinations, T1 was usually chosen at a relatively high temperature in order to obtain the necessary phase transformation fraction. So the nucleation rate is high while the particle shape is mainly spherical because of no time spent at T1. When the temperature is reduced to T2 (especially when T2 is between T_a and T_b), the particle morphology would change with a prolonged calcination time. If the calcination time was located into the shaded domain as shown in Fig. 9, the $Lu_2Ti_2O_7$ particles formed would be spherical with controlled particle sizes. This has been observed in reference 20, in which the holding time was kept at less than 30 minutes. If the calcination time was prolonged beyond the curve 1 and located in the right area of curve 1, the rods formed would grow gradually and in a further step the above referred $Lu_2Ti_2O_7$ nano-wire synthesis mechanism would be triggered again. These small rod-like particles would assemble and result in nano-wires with the help of the crystallization habits of salts under proper conditions. The above referred phenomenon can be observed in references 24 and 25.

Conclusions

The influence of calcination temperature and annealing time on the synthesis of $Lu_2Ti_2O_7$ powders under molten salt conditions was investigated in detail. By controlling the calcination temperature and annealing time, $Lu_2Ti_2O_7$ nano-particles have been successfully obtained via the TSC route based on a molten salt technique. The synthesized $Lu_2Ti_2O_7$ with nano sized particles had a well-defined spherical morphology with no obvious abnormal grown particles found. The distinguishing feature of the TSC method is the precursors used were simple oxides during the synthesis process. So this method is very simple in terms of facilities, easy in manipulation, and has no special requirements for high temperature and/or high pressure. It is rational to expect that this method may be used to synthesize other nano-scaled materials.

References

1. Liliana Mitoseriu, Catalin Harnagea, Paolo Nanni, Appl. Phys. Lett. 84 (2004) 2418-2420.
2. Bin Liu and Hua Chun Zeng, J. Am. Chem. Soc. 125 (2003) 4430-4431.
3. M.-H. Lee, Y.-J. Kang, S.-T. Myung, Y.-K. Sun, Electrochim. Acta 50 (2004) 939-948.
4. Dariusz Bogdal, Piotr Penczek, Jan Pielichowski, Aleksander Prociak, Adv. Polym. Sci. 163 (2003) 51-58.
5. Andrey J. Zarur & Jackie Y. Ying, Nature 403 (2000) 65-67.
6. Changyong Lan, Jiangfeng Gong, Zhiqiang Wang, Mater. Sci. Engineering B 176 (2011) 679-683.
7. Buyin Li, Jia Liu, Yunxiang Hu, J. Alloys. Compd. 509 (2011) 3172-3176.

8. S. Frangini, A. Masci, F. Zaza, Corros. Sci. 53 (2011) 2539-2548.
9. H Tian, Ma J.F, Huang X, Mater. Lett. 59 (2005) 3059-3061.
10. L Li., Shi L.Y., Cao S.M. Mater. Lett. 62 (2008) 1909-1912.
11. X.H Jiang, Ma J.F, Liu J, Ren Y, Lin B.T., Mater. Lett, 61 (2007) 4595-4598.
12. Z.W Song, Ma J.F, Sun H.Y., Ceram. Int. 35 (2009) 2675-2678.
13. X.Y Wang, Zhu Y.P., Zhang W.G., J. Non-Cryst Solids 336 (2010) 1049-1051.
14. H. Tian, Ma. J.F., Xie. L.J., Ceram. Int. 33 (2007) 915-918.
15. A.V. Shlyakhtina, A.E. Ukshe, L.G. Shcherbakova., Russ. J. Electrochem., 41 (2005) 265-269. Translated from Elektrokhimiya 41 (2005) 298-303.
16. Jasbinder Sanghera, Woohong Kim, Colin Baker, Opt. Mater. (2011) 670-674.
17. A.V. Shlyakhtina, A.V. Knotko, M.V. Boguslavskii, Solid State Ionics. 176 (2005)2297-2304.
18. Liqiong. An, Akihiko. Ito and Takashi. Goto, J. Eur. Ceram. Soc. 31 (2011) 237-240.
19. Liqiong. An, Akihiko. Ito and Takashi. Goto, J. Am. Ceram. Soc. 94 (2011) 3851-3855.
20. Bao-rang Li, Nai-qiang Zhang, Hui-bin Chang, Dan Liu. Mater. Lett. 66 (2012) 39-41.
21. T. Kimura, A. Takenaka, T. Mifune, Y. Hayashi and T. Yamaguchi, J. Mater. Sci. 27 (1992) 1479-1483.
22. Baorang li, Hui Gao, Jingjing Liu, Zhiwei Yang, J. Cryst. Growth. 351(2012) 169-175.
23. Baorang li, Huibing Chang, Dongyu Liu, Xiaona Yuan, Mater. Chem. Phys. 130 (2011) 755-759.
24. Baorang li, Hui Gao, Yongquan Guo, Shixiang Hou, Cry Eng Comm. 14 (2012) 4168-4172.
25. Baorang li, Huibing Chang, Hui Gao, Shixiang Hou, Mater. Lett. 79 (2012) 219-221.